Advances in Physics: X

ISSN: (Print) (Online) Journal homepage: https://www.tandfonline.com/loi/tapx20

Time-resolved experiments on gas-phase atoms and molecules with XUV and X-ray free-electron lasers

Daniel Rolles

To cite this article: Daniel Rolles (2023) Time-resolved experiments on gas-phase atoms and molecules with XUV and X-ray free-electron lasers, Advances in Physics: X, 8:1, 2132182, DOI: 10.1080/23746149.2022.2132182

To link to this article: https://doi.org/10.1080/23746149.2022.2132182

Published online: 13 Oct 2022.

ADVANCES IN PHYSICS: X
2023, VOL. 8, NO. 1, 2132182
https://doi.org/10.1080/23746149.2022.2132182

Taylor & Francis
Taylor & Francis Group

REVIEW

Time-resolved experiments on gas-phase atoms and molecules with XUV and X-ray free-electron lasers

Daniel Rolles

J. R. Macdonald Laboratory, Department of Physics, Kansas State University, Manhattan, KS, USA

ABSTRACT

Over the last 20 years, XUV and X-ray free-electron lasers have enabled a wide variety of time-resolved experiments that have dramatically advanced our understanding of ultrafast molecular dynamics on atomic length scales and femtosecond time scales. This review focuses on experimental studies of ultrafast dynamics of atoms and molecules in the gas phase, tracing the development of the field from early proof-of-principle studies to recent pump-probe experiments that elucidate the coupled electronic and nuclear dynamics during photochemical reactions with a temporal resolution that is now extending into the attosecond domain.

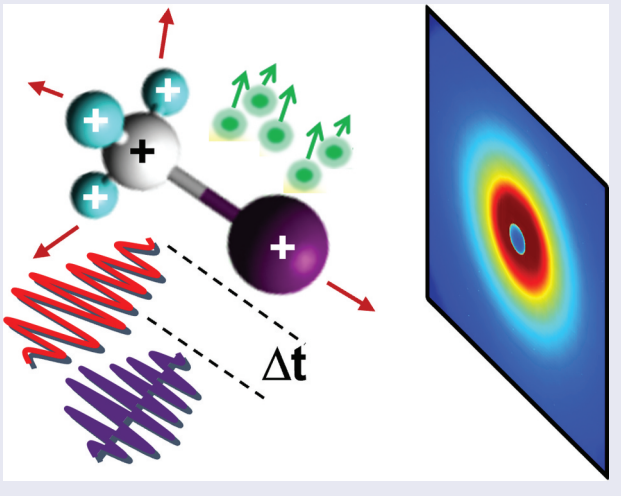

ARTICLE HISTORY
Received 28 March 2022
Accepted 27 September 2022

KEYWORDS
Free-electron lasers; atomic and molecular physics; time-resolved; pump-probe

I. Introduction

Free-electron lasers (FELs) are accelerator-based light sources that can produce short and intense light pulses over a wide wavelength range from microwaves to the extreme ultraviolet (XUV) and X-ray regime [1–17]. This has made it possible to extend the thriving field of femtochemistry –

CONTACT Daniel Rolles rolles@phys.ksu.edu J. R. Macdonald Laboratory, Department of Physics, Kansas State University, Manhattan, KS 66506, USA

pioneered by Nobel Laureate Ahmed Zewail in the near-infrared, visible, and ultraviolet wavelength range [18] – to shorter wavelengths that are amenable to site- and element-specific spectroscopy applications and atomic-resolution imaging experiments. Furthermore, using XUV or X-rays for either pump or probe pulse (or both) allows for single-photon excitation or ionization, which often simplifies the theoretical description considerably as compared to using a multiphoton or strong-field process for the pump and/or probe step, as done in many 'traditional' femtochemistry experiments.

In an XUV or X-ray FEL – often also abbreviated as XFEL -, electron pulses produced by irradiating a photocathode with short optical or ultraviolet laser pulses (some XFELs also use a thermionic cathode) are accelerated to relativistic energies in a linear accelerator. The resulting beam or 'train' of electron bunches, each tens to hundreds of femtoseconds in duration, are sent through a strong magnetic field generated by an array of magnets with alternating poles called undulator, that forces the electron bunches on an oscillating, sinusoidal trajectory. The oscillating relativistic electron bunches produce powerful XUV or X-ray pulses known as synchrotron radiation. If the undulator is long enough, the electric field of the synchrotron radiation interacts with the co-propagating electron bunches, causing a (longitudinal) modulation of the electron density in each bunch with the same period as the driving light field. The electrons in the resulting microbunches continue to emit further XUV or X-ray photons that are coherent with the originally emitted radiation, and the consequence is a strong amplification of that radiation through a process known as self-amplified spontaneous emission (SASE) [1,4,9]. Alternatively, an external 'seed' laser field can be overlapped with the electron bunches in the undulator, causing the seed pulses to be coherently amplified and thus producing intense XUV or X-ray pulses with a much improved temporal coherence as compared to those generated by a SASE process [4,6,9]. A combination of both schemes, called 'self-seeding', uses the monochromatized SASE radiation produced in an early part of the undulator to seed the amplification process in the latter part of the undulator [19]. In all of these cases, the result are strong, femtosecond XUV or X-ray pulses with laser-like characteristics that can be focused to a spot size of few micrometers or below, which are ideally suited for time-resolved experiments.

In the following, several examples of time-resolved experiments with FELs in the field of atomic, molecular and optical (AMO) physics and gas-phase physical chemistry are presented. Given the two decades of experimental activity in this area, this short review can only highlight a subset of the relevant work that has been performed to date. The examples that were selected attempt to showcase the historic development of the field: from early proof-of-principle experiments that were primarily designed to

characterize the FEL pulses and to develop and refine the technical capabilities for pump-probe experiments, to more recent studies aimed at elucidating electronic and nuclear dynamics during photochemical reactions, including very recent developments that have pushed FEL pump-probe experiments into the attosecond regime.

II. Pump-probe schemes

Most time-resolved experiments with FELs are performed in a pump-probe scheme using a first pulse (the 'pump' pulse) to trigger the reaction of interest, and a second pulse (the 'probe' pulse) to interrogate the state of the system at a series of time delays that can range from hundreds of attoseconds to hundreds of picoseconds or more, depending on the time constants of the process. Such a pump-probe scenario can be achieved in several ways: by splitting the FEL pulse into two pulses whose relative timing with respect to each other can be controlled with high precision; by generating two (or more) XUV or X-ray pulses with variable time delay in the undulator, either from one or several electron bunches; or by synchronizing an external laser source, such as a tabletop (near-)infrared laser, to the FEL with high temporal precision and minimum timing jitter. All of these experimental schemes are commonly employed, each with their own benefits and technical challenges that will briefly be discussed in the following.

A. XUV–XUV and X-Ray–X-Ray pump-probe schemes

Most pump-probe schemes in the ultraviolet (UV), visible, and near-infrared (NIR) rely on a beam splitter to split a single laser beam into two paths. In each path, the pulses can be manipulated further and their relative timing with respect to each other can be adjusted, e.g. via a delay stage, before they are recombined in order to be used as pump and probe pulses. Common optical beam splitters either use a semitransparent mirror that allows a certain fraction of the laser pulse to be transmitted while the other part is reflected, or they use a split mirror that cuts the wave front of the incoming pulse into two parts that can be used as pump and probe pulses. Extending these schemes to the XUV and X-ray domain poses some technological challenges since semitransparent beam splitters are not readily available, and most X-ray mirrors need to be used in grazing incidence, i.e. at very shallow angles, in order to achieve high reflectivity. This requires rather large and cumbersome beam paths in order to achieve wave front splitting and adjustable delays. Nevertheless, such grazing-incidence split-and-delay setups have been realized both in the XUV [20–22] and X-ray range [23]. In the XUV domain, an alternative to grazing-incidence mirrors are normal-incidence multilayer mirrors that can also achieve high

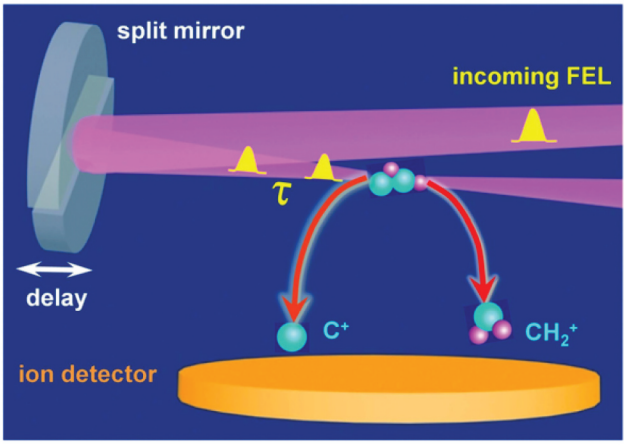

Figure 1. Schematic of a normal-incidence split-mirror setup for XUV pump-probe experiments. The incoming XUV beam is backfocused by an (in-vacuum) normal-incidence multilayer mirror that is cut into two halves. One of the halves is movable, e.g. using a piezo stage, such that the incoming XUV pulse is split into two pulses with variable delay. The relative intensity of each pulse can be adjusted by moving the mirror perpendicular to the beam direction such that more or less than half of the beam is reflected by the movable part. Figure taken from [108].

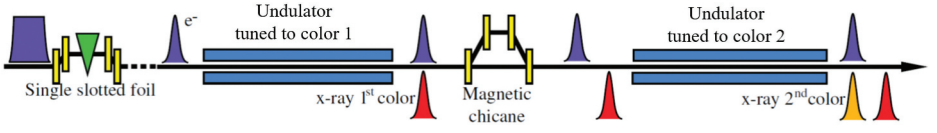

Figure 2. Generation of two-color, few-femtosecond X-ray pulses. A few-femtosecond electron bunch, generated, e.g. using a slotted foil (green upside-down triangle), produces a few-femtosecond X-ray pulse in the first part of the undulator. A magnetic chicane introduces an adjustable delay between the X-ray pulse and the electron bunch, which then loses again at a different color in the subsequent part of the undulator section. An alternative approach uses two electron bunches produced at the photocathode, each of which loses only in one of the two undulator sections. Figure adapted from ([27]).

reflectivity and allow a more compact split-mirror design [24–26], as shown, e.g. in Figure 1. However, these multilayer mirrors only have high reflectivity at one (or a few) chosen wavelength(s), thus requiring fabrication and installation of a new mirror for each experiment that is performed at a different photon energy.

Recently, new schemes for X-ray – X-ray pump-probe experiments have emerged based on the generation of two independent X-ray pulses with controllable delay by the FEL itself [27–30], as shown in Figure 2. The big advantage of these schemes is that they avoid the often quite substantial transmission losses caused by the additional mirrors in split-and-delay units, and that depending on the exact details of the generation scheme, it is possible to produce two pulses with different photon energies, which opens up a new class of two-color pump-probe experiments. For example, by tuning the photon

energies of the two pulses below and above an inner-shell absorption edge, respectively, this scheme enables site-specific pump-probe experiments, where the pump and probe pulse are selectively absorbed by two different atoms inside the molecule [31]. Similar two-color schemes have been developed for the XUV and soft X-ray regime and have been used, e.g. for coherent control experiments that take advantage of the longitudinal coherence of the seeded FERMI FEL and the ability to generate phase-stable pulse pairs [32–35]. These developments may open up exciting new opportunities for nonlinear X-ray optics [36] and multidimensional X-ray spectroscopy [37], as briefly discussed in section IV.

B. Pump-probe schemes with synchronized external laser pulses

While using two XUV or X-ray pulses, produced either by splitting a single pulse or by generating two pulses in the photocathode or FEL undulator, allows pump-probe experiments with minimal temporal jitter that can reach few- to sub-femtosecond temporal resolution, a large class of pump-probe experiments requires pulses in the ultraviolet, visible, or infrared spectral region for manipulating the target, e.g. to excite a specific electronic transition in a neutral atom or molecule (see section III D), or to align an ensemble of target molecules via adiabatic or impulsive laser-alignment techniques (see section III B). This is typically achieved by synchronizing an external laser to the FEL and by spatially and temporally overlapping those external laser pulses with the FEL pulses on the target [38], which is usually inside a vacuum chamber for most AMO experiments, as shown schematically in Figure 3.

The biggest challenge here is the precise synchronization of the external laser with the FEL, since the latter usually extends over several hundred meters to a few kilometers – from injector laser and photo cathode to the

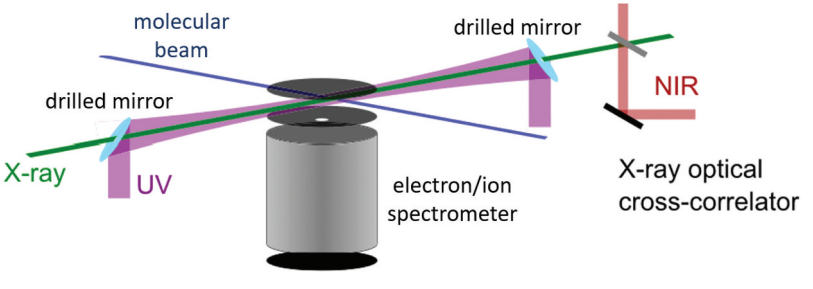

Figure 3. Sketch of a typical pump-probe setup combining X-rays and external laser pulses. The external laser beam (here: in the UV) is coupled in collinearly to the X-ray beam via a drilled mirror. Both beams are focused onto a supersonic molecular beam, and the resulting electrons or ions are detected by a time-of-flight or imaging spectrometer. Downstream of the interaction region, the arrival time jitter between the FEL and the external laser pulses is recorded by an X-ray/optical cross-correlator. Figure adapted from [89].

experimental end-station – such that even the smallest temperature fluctuations will result in temporal drifts of hundreds of femtoseconds or more. Sophisticated synchronization and locking schemes have been developed to reduce the resulting temporal pulse-to-pulse jitter and longer-terms drifts to tens of femtoseconds [15,39–42]. Nevertheless, most of the early pump-probe experiments with FELs that relied on external lasers were limited to an effective temporal resolution of several hundred femtoseconds.

To overcome these practical limitations, various X-ray/optical cross-correlators and bunch arrival monitors have been developed to measure the relative arrival-time jitter between the FEL and the external laser pulses or another external master clock on a shot-by-shot basis (see Ref [43]. for an extensive list of references). This provides the ability to correct for the shot-by-shot timing jitter by sorting the external data through post-analysis, thereby allowing pump-probe experiments with external lasers with an effective synchronization of tens of femtoseconds or better [43,44].

Another scheme for X-ray – optical pump-probe experiments relies on externally seeding the FEL and on using the seed laser as an optical pump or probe laser, as it is realized, e.g. at the FERMI facility [6]. In this case, the intrinsic synchronization between the seed laser and the seeded FEL pulses significantly reduces the timing jitter.

Finally, a third alternative that is almost completely free of temporal jitter relies on the use of an additional undulator to generate (far-)infrared radiation by the same electron bunch that has produced the FEL radiation. The radiation from this far-infrared undulator can even be phase-stable with respect to the XUV or X-ray pulses, thereby allowing pump-probe experiments with extremely high temporal resolution, especially using the terahertz streaking technique [45] (see also Figure 5).

III. Femtosecond pump-probe experiments with free-electron lasers

A. Two-color experiments for pulse characterization

Since the temporal profile and pulse duration of FEL pulses produced by self-amplified spontaneous emission (SASE) is difficult to predict accurately and varies wildly on a shot-by-shot basis [9], one of the objectives of many of the early pump-probe experiments with FELs was the temporal characterization of the femtosecond XUV and X-ray pulses (see, e.g. Refs. [46–48] for early reviews). Often, these experiments were inspired by methods developed in the strong-field community for the characterization of femtosecond and attosecond XUV pulses produced by high harmonic generation.

A direct and relatively simple way to determine the cross correlation between a femtosecond optical (often near-infrared) pulse and the FEL pulse – and, thus, the pulse duration of the FEL pulse (assuming the

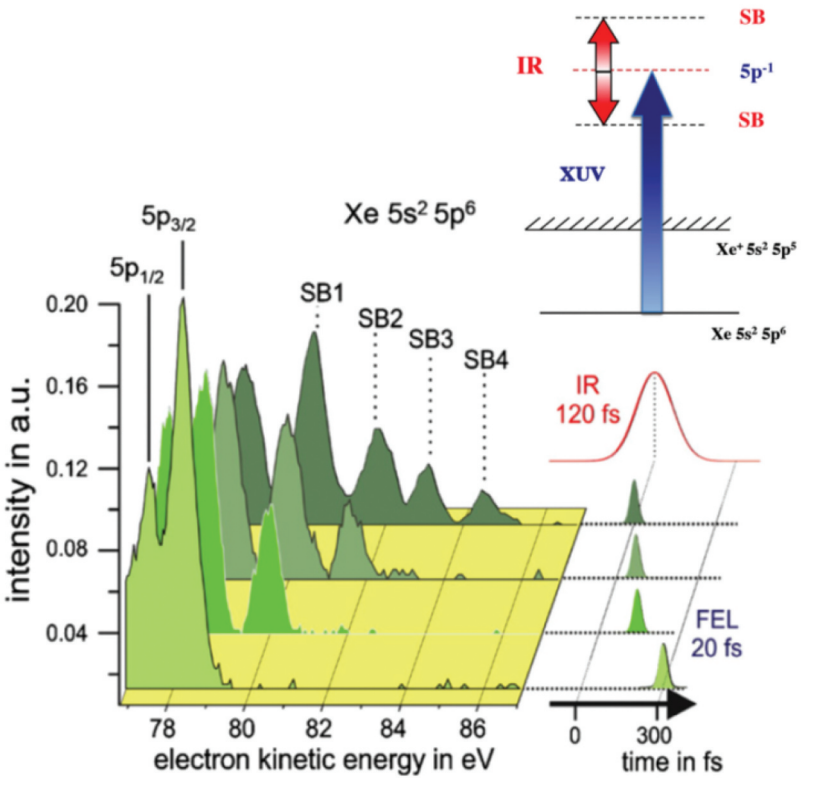

Figure 4. Sidebands in the Xe(5*p*) photoelectron spectrum recorded at a photon energy of 90.0 eV as a function of delay between the FEL and 800-nm NIR pulses. The inset shows a schematic representation of the two-color ATI process for 5*p* ionization of atomic Xe. Figure adapted from [47].

duration of the optical pulse is known) – is by measuring 'sidebands', or two-color Above Threshold Ionization (ATI), in the photoelectron spectrum of rare-gas atoms, as shown in Figure 4. In the presence of an intense NIR laser pulse, the photoelectron produced by the FEL pulse can absorb additional NIR photons, which results in several side peaks to the main photoline, each spaced one NIR photon apart, similar to an ATI spectrum produced by laser-atom interaction in the multiphoton regime. The first sideband experiments with FELs were performed at FLASH [47–55] and shortly thereafter at LCLS [56], and exemplary results are shown in Figure 4.

A more complete characterization of the FEL pulse, in particular a direct measurement of its pulse profile, is possible via streaking measurements, again in close analogy to similar experiments performed with HHG [57]. Since the FEL pulses are typically longer than one optical cycle of a near-infrared laser, mid-IR or THz stretching fields are best suited for such experiments. Furthermore, because of the above-mentioned jitter between the FEL and external laser pulses, the two are not phase stable (as is usually

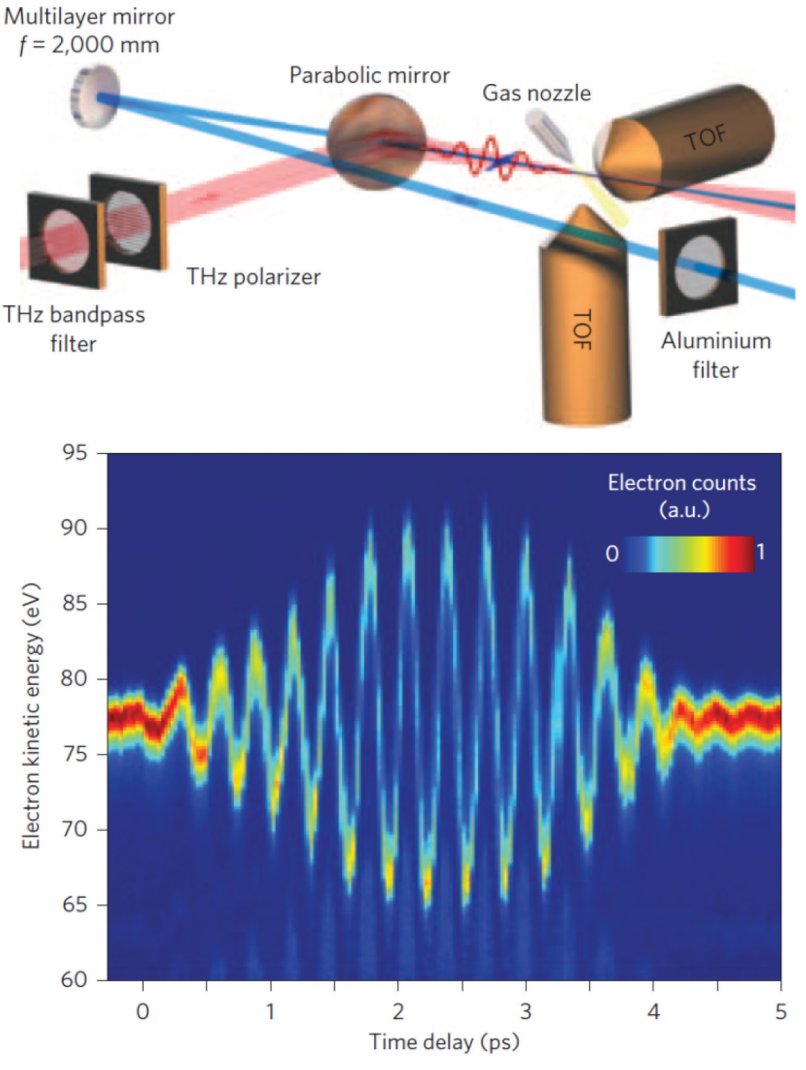

Figure 5. Schematic of the experimental setup for a THz streaking experiment at FLASH (top) and the corresponding streaking trace (bottom) recorded as a series of kinetic energy spectra of Kr(4*p*) photoelectrons produced by a 13.5-nm FEL pulse in the presence of an intense THz field. The energy shift of the electrons as a function of the delay directly represents the vector potential of the THz field. Figure adapted from [45].

the case for HHG streaking experiments), so the experiment needs to also determine the phase on a shot-by-shot basis and sort the data accordingly [58–61]. A beautiful way to circumvent this problem was developed at FLASH, where the electron beam used to generate the XUV pulse in the FEL undulator can be sent through an additional undulator that generates intense far-infrared/THz pulses that are phase stable with the FEL and can be used, e.g. for streaking experiments [45,62,63], as shown in Figure 5

As an alternative to the above techniques for pulse characterization, all of which rely on measuring some form of cross correlation with an external laser or THz source, several autocorrelation measurements have been performed with FEL pulses [21,24,48,64,65]. These require splitting the FEL pulse via specialized XUV or X-ray beamsplitters or split and delay units, as described in section II A.

B. Experiments on laser-aligned molecules

Inspired by sophisticated methods for laser-aligning gas-phase molecules developed in ultrafast laser laboratories around the world (see Ref [66]. for a comprehensive review), several experiments have attempted to transfer and adapt these methods for FEL experiments and to exploit the additional information available through the ensuing measurements in the molecular

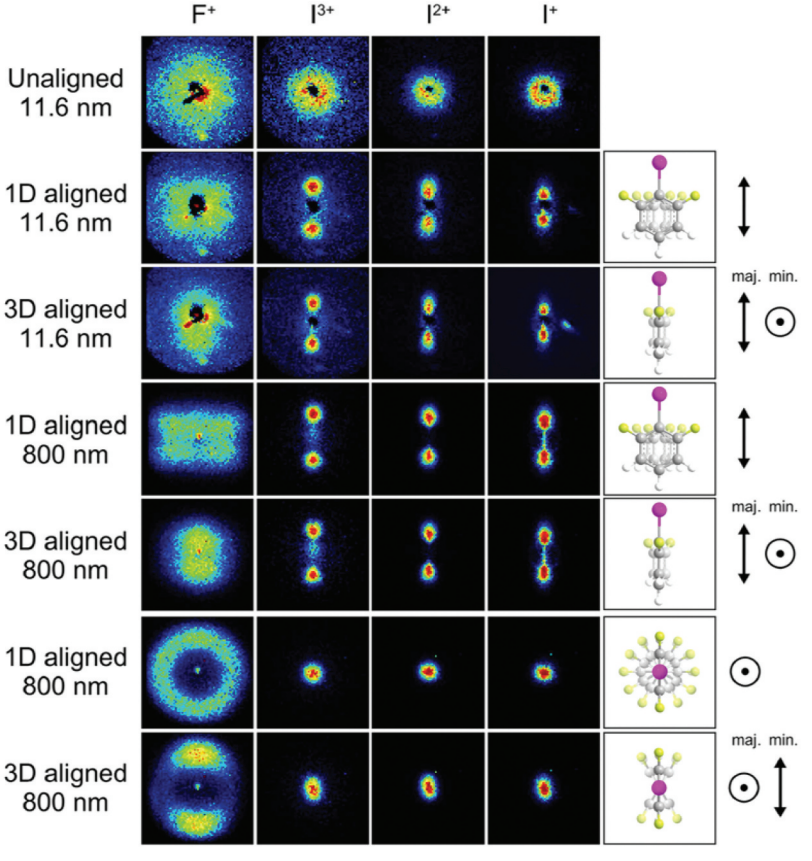

Figure 6. Fragment-ion angular distributions of adiabatically laser-aligned difluoroiodobenzene molecules probed by intense 11.6-nm (107 eV photon energy) FEL pulses as well as by strong-field ionization with an 800-nm laser pulse. The ion images were recorded with a velocity map imaging spectrometer. Figure adapted from [74].

frame. Many of the early experiments of this type [39,67–69] used an impulsive alignment scheme, which allows an experiment on aligned molecules under field-free conditions (i.e. in one of the so-called revivals of the rotational wavepackets; see Ref [66].) but, in practice, often only provided a rather low degree of alignment. Other experiments obtained a higher degree of alignment (see Figure 6) by employing an adiabatic alignment scheme using nanosecond laser pulses [70–76], albeit at the expense of having a strong laser field present during the measurement. This turned out to be particularly problematic for experiments aimed at using photoelectron diffraction to probe molecular dynamics [70,72,73] since the strong laser field led to a broadening of the photoelectron lines, and it was also concluded that ionization or dressing of excited states may alter the molecular dynamics of interest [73,77,78].

Other photoelectron diffraction experiments therefore employed impulsive alignment but suffered from the low degree of alignment that washed out most of the diffraction structure [79–81], while more recent experiments aimed at investigating molecular-frame photoelectron angular distributions employed electron-ion coincidence techniques [82,83] enabled by higher-repetition-rate FELs such as the European XFEL. With the projected increase of the available XFEL repetition rates by another three orders of magnitude at LCLS-II [84], electron-ion coincidence methods are expected to become increasingly important and will significantly enhance the information that can be obtained from time-resolved electron and ion spectroscopy experiments, as outlined further in section IV.

C. Inner-shell ionization and charge transfer dynamics

By choosing an appropriate photon energy, the site- and element specificity of the inner-shell X-ray absorption process can be used to create a highly localized (core) hole in a polyatomic molecule. After Auger-Meitner decay of the core hole, which leads to two or more holes in the valence shell, this positive charge is often still highly localized before it starts spreading over the molecule via a charge transfer mechanism [85]. Inner-shell ionization or excitation is therefore well suited for initiating intramolecular charge transfer that can then be probed in a time-resolved experiment. A sketch of such an inner-shell pump-probe experiment studying charge transfer in a CH_3I molecule is shown in Figure 7. At the photon energy of 1.5 keV employed in this experiment [86], photoabsorption occurs almost exclusively on the iodine atom via ionization of the I(3*d*) shell. An Auger-Meitner cascade then leads to a multiply charged molecular final state, which breaks up via Coulomb explosion after some of the positive charge has been transferred to the methyl group. In order to investigate how this charge transfer between the iodine atom and the methyl group depends on the distance between

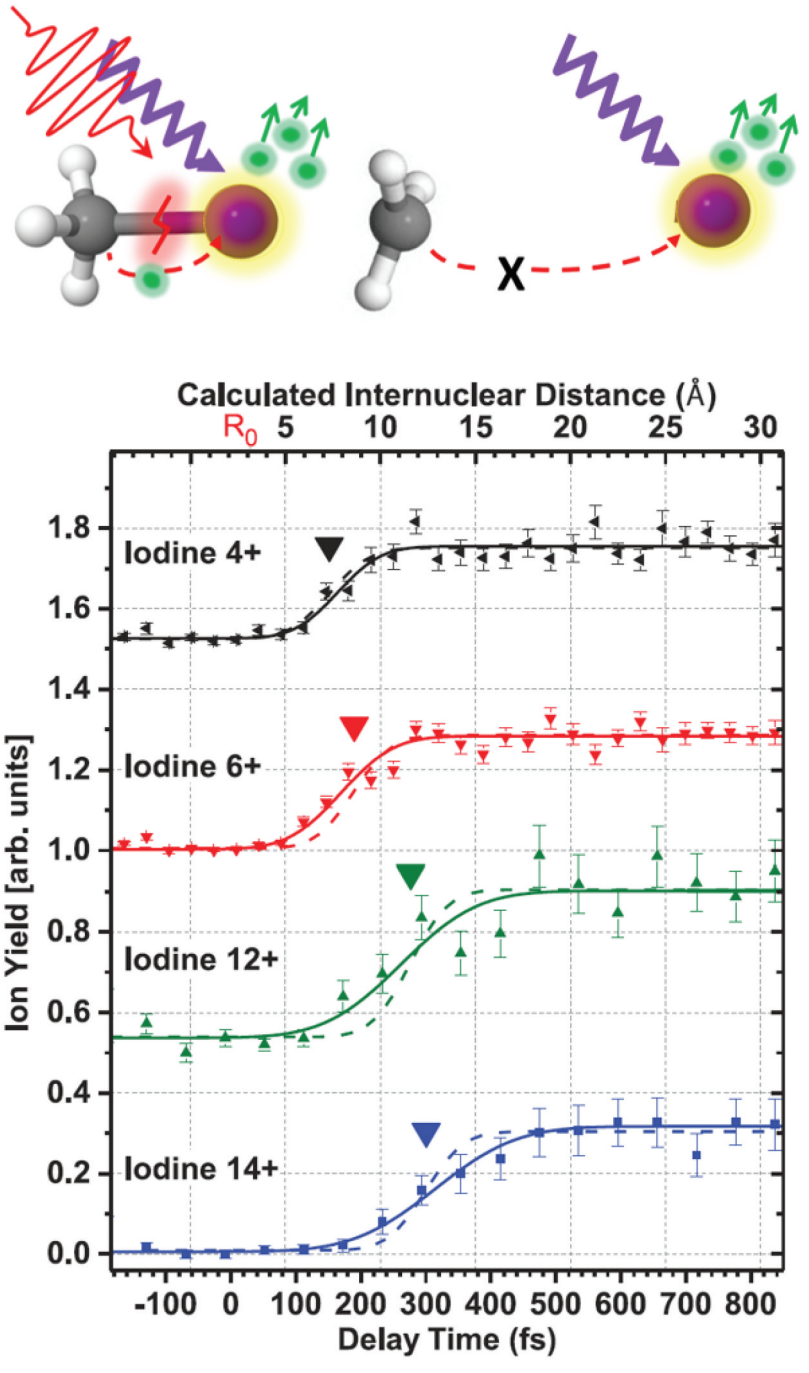

Figure 7. Schematic illustration of an NIR-pump–X-ray probe experiment on CH_3I investigating the distance dependence of intramolecular charge transfer. The bottom panels shows the delay- and distance-dependent yield of low-energy iodine ions (see text). Figure adapted from [86].

these two moities, the pump-probe experiment used an additional near-infrared laser pulse to dissociate the molecule prior to the arrival of the X-ray pulse. Since the dissociation velocity is well known, the time delay between the NIR and X-ray pulse is therefore (to good approximation) linearly related to the distance between the iodine and the methyl fragment. At small delays and, thus, small internuclear distance, some of the positive charge created on the iodine atom after X-ray ionization can easily transfer to the methyl group (in practice, it is actually one or more electrons from the methyl group that transfer to the iodine atom to refill some of the valence holes), and the molecule will Coulomb explode. However, if at a later delay, the internuclear distance is larger than a certain 'critical distance', charge transfer is no longer possible, and all the positive charge stays localized on the iodine atom. In that case, the experiment will detect a highly charged iodine ion with small kinetic energy due to the lack of Coulomb explosion. The bottom panel of Figure 7 shows the yield of these low-energy iodine atoms as a function of delay (bottom axis) and internuclear distance (top axis). A step-like increase in the yield can be seen at a certain internuclear distance that increases with the iodine charge state, in good agreement with the predictions from a classical over-the-barrier charge transfer model, shown as upside down triangles.

Similar charge transfer studies were also performed after I(4*d*) ionization [87,88], on UV-dissociated CH_3I using both I(3*d*) [89]and I(4*d*) ionization [90–92], as well as on I_2 [93,94], CH_2IBr [95,96], and difluoroiodobenzene [43,90]. Furthermore, it was recently shown that intramolecular charge transfer can also be probed by ultrafast X-ray scattering, as demonstrated for the case of N,N'-dimethylpiperazine [97]. Finally, as a direct extension of experiments performed with attosecond and few-femtosecond HHG sources, ultrafast electronic dynamics in atoms and molecules were recently also studied by FEL-based transient absorption experiments [98,99].

D. Photochemistry

Many time-resolved experiments on gas-phase molecules that are conducted with FELs fall into the realm of (gas-phase) photochemistry, i.e. their goal is to study ultrafast light-induced chemical reactions such as photodissociation and isomerization processes. These reactions are often induced by photoabsorption into a neutral excited state and may involve transition through one or several conical intersections leading to the formation of the photoproducts; or they may occur on cationic or di-cationic potential energy surfaces and, thus, need to be triggered by photoionization. Investigations of light-induced dynamics in neutral molecules almost always requires a pump-probe arrangement with a synchronized external laser (see section II B), which is often converted into the visible or ultraviolet by non-

linear wavelength conversion. Dynamics in ionic states can often also be probed by an XUV–XUV or X-ray–X-ray pump-probe scheme, as discussed in section II A. Either one of these pump-probe schemes is then combined with photoelectron or ion spectroscopy or a photon-in photon-out technique such as X-ray absorption, X-ray emission spectroscopy, or X-ray scattering in order to detect a time-dependent signal from which information about the process of interest can be derived.

Since such gas-phase photochemistry experiments with FELs have experienced an explosion in popularity in recent years, only a few examples of the different flavors of such experiments will be highlighted in the following, and the interested reader is referred to the references for further perusing.

1. Time-resolved ion mass spectrometry and ion imaging

Time-resolved mass spectrometry is a well-established technique for ultrafast photochemistry studies with table-top laser sources, which is easily applicable to FEL experiments. In addition to one of the pump-probe schemes discussed in section II, it only requires a simple ion time-of-flight

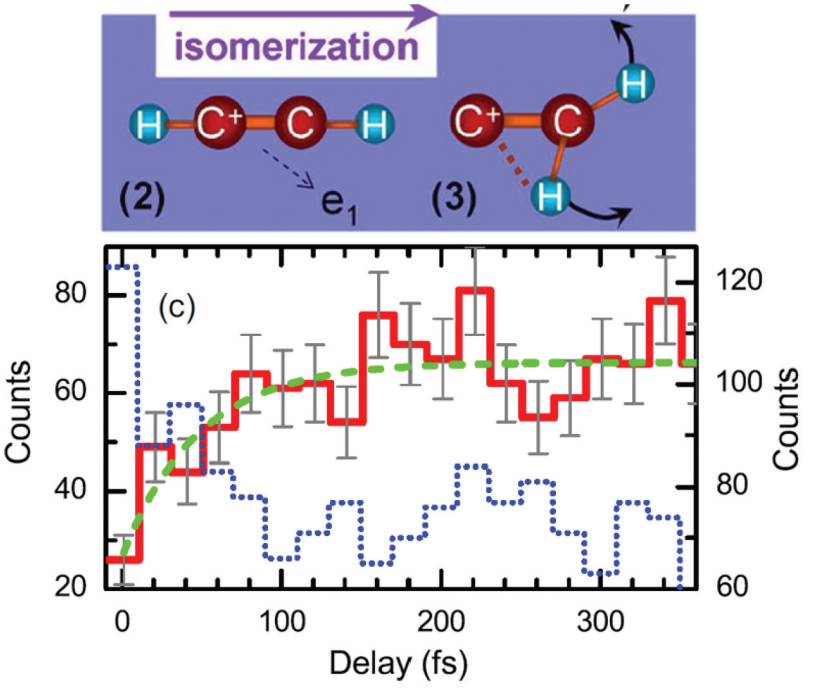

Figure 8. Sketch of the isomerization reaction of an acetylene cation created by XUV ionization. The bottom panel shows the yield of C^+ and CH_2^+ fragments detected in coincidence (solid red line) after a second XUV pulse ionizes the molecule a second time. The dashed green line is a fit of an exponential function to the data, and the dotted blue line shows the yield of C^{2+} and C^{2+} fragments detected in coincidence (right y axis), which represents an autocorrelation signal. Figure adapted from [109].

spectrometer, which was available in most of the early FEL end-station (see Refs. [100,101] for early reviews). However, significantly more information on the reaction of interest can be obtained from ion imaging experiments that record the kinetic energy and angular distribution (or sometimes also the full three-dimensional momentum information) of the emitted fragment ions, which, in some cases, are even detected in coincidence. Most of the experiments described in section III C were performed using various forms of time-resolved ion imaging. Other examples include experiments on neon dimers [102], argon clusters [103], and studies of ultrafast electronic relaxation [104], molecular dissociation [69,105,106], and isomerization reactions, e.g. in cyclohexadiene [107] or acetylene [108–110], as shown in Figure 8. In the example shown here, a first XUV pulse was used to ionize the acetylene molecule and trigger the isomerization reaction from the H-C-C-H to the C-C-H_2 geometry. The formation of the latter was probed by recording the yield of C^+ and CH_2^+ fragments detected in coincidence after a second XUV pulse ionizes the molecule a second time. Other time-resolved ion spectrometry experiments using the XUV – XUV and X-ray – X-ray pump-probe schemes described in Section II A include studies on D_2 [111], N_2 [24,112], Ne_2 [113], XeF_2 [31], CH_3I [114], fullerenes [115], and Xe clusters [116].

While several of the experiments mentioned here were performed in an ion-ion coincidence mode, the development of high-repetition-rate FELs such as the European XFEL [16] and LCLS-II [84] will dramatically decrease the acquisition times required for multi-particle coincidence experiments detecting three or more ions [117–119], which makes multi-ion coincidence techniques promising candidates for future time-resolved experiments.

2. Time-resolved photoelectron spectroscopy

Similar to time-resolved mass spectrometry, which is discussed right above, time-resolved photoelectron spectroscopy (TRPES) is a commonly used technique for femtochemistry studies with table-top laser sources [120]. Applying TRPES to FELs has several advantages: Using an XUV or X-ray FEL pulse for the probe step allows for site- and element-specific probing via inner-shell ionization. And when probing via valence ionization, using a photon energy above the ionization potential of the target molecule and the possible photoproducts makes it possible to follow the molecular dynamics not just in the electronically excited state but also subsequent dynamics on the electronic ground state, which cannot be ionized by a single-photon absorption in the visible or UV domain. In principle, both of these advantages also apply to TRPES with HHG sources, but the lower photon flux of most HHG sources often poses a practical challenge for gas-phase TRPES studies, both for valence photoelectron spectroscopy but especially for inner-shell photoelectron spectroscopy. A drawback and

direct consequence of the high pulse energies at FEL sources, however, is the need to (often severely) attenuate the pulses in order to minimize multi-photon ionization and, in particular, to minimize broadening of the electron spectra due to space charge effects (i.e. to avoid the simultaneous generation of too many electrons in the interaction region, which would lead to substantial spectral broadening). Nevertheless, the acceptable count rates of several tens to hundreds of electrons per shot still exceeds by far the count rates that can be achieved in typical HHG-based experiments, thus giving the FEL experiments a clear edge over HHG experiments performed at comparable repetition rates.

Examples for time-resolved inner-shell photoelectron spectroscopy experiments with FELs include studies of the UV-induced dissociation of $Fe(CO)_5$ [121] and CH_3I [91], measurements of excited-state chemical shifts [122], the photoelectron diffraction experiments mentioned in section III B, as well as time-resolved Auger electron spectroscopy [123] and X-ray absorption measurements [124], as shown in Figure 9. Here, the electronic and nuclear dynamics of the nucleobasis thymine after UV excitation were probed locally via inner-shell ionization and subsequent Auger-Meitner decay of a highly localized core hole on the oxygen atom. The time-dependent Auger-Meitner spectrum shows an immediate blue shift right after photoexcitation (see region I in the right panel of Figure 9), that is interpreted as a signature of a C-O bond stretch upon photoexcitation on a timescale faster than the instrument response function. On a longer time

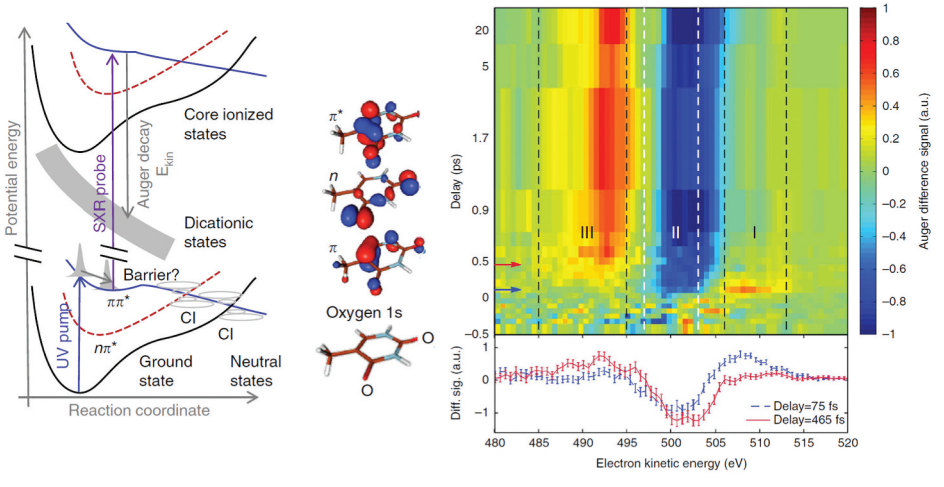

Figure 9. Sketch of the UV-pump soft-X-ray-probe scheme applied to thymine (left). The electronic and nuclear dynamics induced by UV photoabsorption, which excites the molecule to the $\pi\pi^*$ state, are probed by measuring the Auger-Meitner spectrum following oxygen 1s core-shell ionization in a magnetic bottle electron spectrometer. The panel on the right shows the difference between the Auger-Meitner spectrum with and without UV excitation as a function of pump-probe delay. Figure adapted from ([123]).

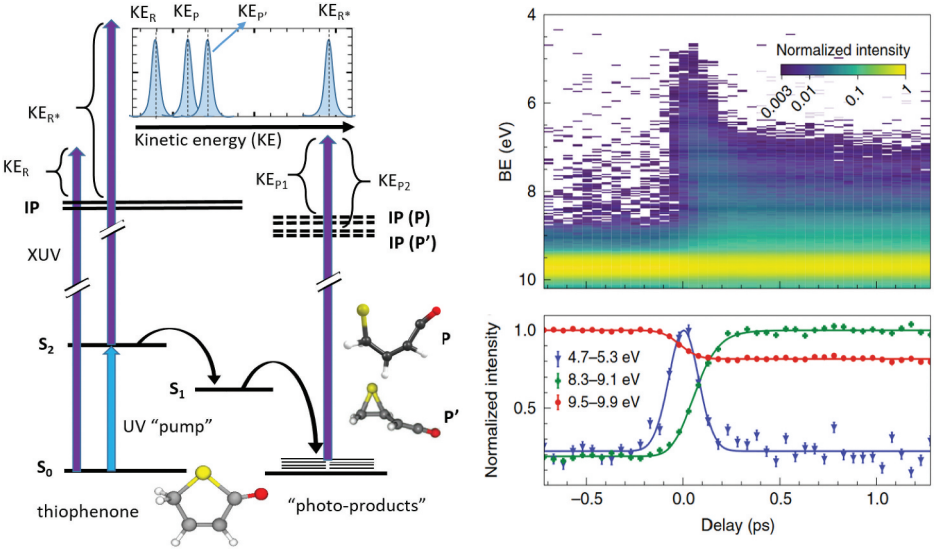

Figure 10. Sketch of a UV-pump XUV-probe TRPES experiment on thiophenone (see text). The panel on the right shows the photoelectron spectrum in terms of binding energy (BE), cut right below the outermost-valence level, as a function of pump-probe delay, along with line-outs of the time-dependent photoelectron signal in the BE regions corresponding to ground-state thiophenone (red), photoproducts (green), and thiophenone in the S_2 excited state (blue). Figure adapted from ([125]).

scale, a red shift of the spectrum into region III is observed and attributed to population transfer from the $\pi\pi^*$ to the $n\pi^*$ state with a time constant of approximately 200 fs.

In contrast to the site-selective probing by soft X-ray core ionization in Figure 9, Figure 10 shows an example of FEL-based valence-shell TRPES. Here, the electronic relaxation and ring-opening dynamics of gas-phase thiophenone following UV excitation are probed by monitoring the change of the outer-valence spectrum, as shown in the sketch on the left-hand side of Figure 10. Photoemission from the electronically excited reactant molecule R* in the S_2 state leads to a photoelectron signal that is upshifted in kinetic energy with respect to the reactant molecule in the S_0 ground state. During the electronic decay through the S_1 state, which is coupled to large-scale nuclear motion along the C-S ring-opening coordinate, the photoelectron intensity shifts gradually towards lower kinetic energy. It eventually reaches a new steady state corresponding to photoemission from the vibrationally hot ring-opened products P and P' in their electronic ground states. This transient upshift of the photoelectron spectrum towards higher kinetic energy (i.e. lower binding energy), along with a depletion of the signal from ground-state thiophenone (red circles in the bottom panel) right at zero time delay, followed by a sweep of the photoelectron intensity towards higher binding energy is also seen in the experimental data shown on the

right-hand side of Figure 10. The associated time scales are in good agreement with *ab initio* molecular dynamics calculations [125].

A few years prior to the experiment shown in Figure 10, a similar valence-shell TRPES study was performed on UV-excited acetylacetone, probing the coupled electronic and nuclear dynamics on a time scale of several hundred femtosecond to tens of picoseconds [126]. Both of these experiments were done with a seeded FEL [6], which provides a much narrower spectral bandwidth than other FEL facilities that are based on SASE. This is particularly crucial for photoelectron spectroscopy since the photon energy bandwidth (and photon energy jitter), which are typically on the order of 0.5% to 1% for SASE FELs, directly affect the spectral resolution of the measurement. However, a new type of correlation analysis dubbed 'spectral domain ghost imaging' was shown to alleviate this limitation, thus opening the door for high-resolution photoelectron spectroscopy also with SASE-based FELs [127–129]. The method requires a simultaneous high-resolution measurement of the fluctuating XUV or X-ray spectrum for each FEL pulse along with recording the shot-by-shot photoelectron spectrum and uses the statistical correlation between the two to achieve sub-bandwidth spectral resolution in the photoelectron spectrum.

3. *Ultrafast X-ray scattering*

Even though ultrafast X-ray scattering and coherent diffractive imaging on solids, liquids, nanocrystals, nanoparticles, and clusters [130–133] have been hallmarks of XUV and X-ray FELs since their inception, the application of these techniques to gas-phase photochemistry applications is

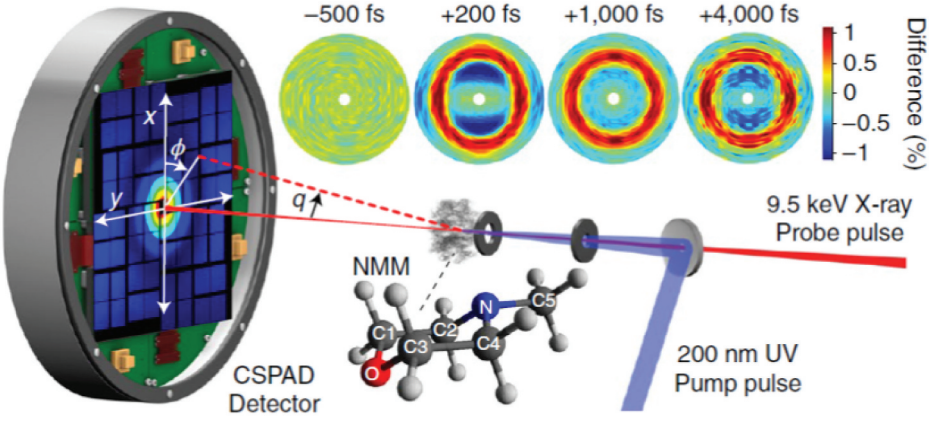

Figure 11. Schematic of a gas-phase ultrafast X-ray scattering experiment on N-methylmorpholine (NMM). The molecules interact with the UV-pump pulse and the hard-X-ray probe pulse in a windowless gas cell inside a vacuum chamber, and the time-resolved scattering images are recorded with a large-area X-ray imaging detector. The insets show difference images of the scattering patterns at several time delays. Figure taken from ([136]).

a relatively new addition to the portfolio of time-resolved FEL experiments. While some initial X-ray scattering experiments were performed on laser-aligned molecules in supersonic molecular beams [71,76], the vast majority of time-resolved experiments use much denser targets in a gas cell to achieve the signal levels required for ultrafast high-resolution X-ray scattering [134–138].

The molecular systems studied with ultrafast X-ray scattering to date range from diatomics such as vibrationally excited and dissociating I_2 [135,138] to organic ring molecules such as cyclohexadiene [134,137,139] and other organic molecules with close to 20 atoms or more, such as N,N'-dimethylpiperazine [97] and N-methylmorpholine [136], as shown in Figure 11. In these most recent experiments, bond distances were determined with 0.01-Ångström precision, and different product geometries as well as signatures of coherent vibrational motion and charge transfer were identified [97,136].

IV. Future perspectives

While time-resolved experiments with FELs have made tremendous progress over the last two decades, exciting new opportunities continue to arise as the capabilities of the FEL sources continue to evolve [140,141]. For example, the demonstration of attosecond soft and hard X-ray pulses at LCLS [60,142,143] and single-spike SASE operation in the XUV [62] will enable new experiments studying ultrafast electron and hole dynamics, which have, so far, been primarily conducted with HHG sources. Indeed, recent experiments at FLASH and LCLS used X-rays to create and monitor correlated electron dynamics in inner-shell ionized argon atoms [65], electronic wave packets in an amino acid glycine [144], electron hole dynamics in isopropanol [145]; and electronic population transfer via impulsive stimulated X-ray Raman scattering with attosecond soft-X-ray pulses [146]. Attosecond X-ray pulses were also used to clock the emission of Auger-Meitner electrons in neon [61] and to probe attosecond coherent electron motion during Auger-Meitner decay in nitric oxide [147]. Along with new schemes for generating phase-stable XUV and X-ray pulse pairs [32–36], these developments may enable the application of coherent (multi-dimensional) spectroscopy at FELs for dynamic studies in the gas phase, as suggested, e.g. in pioneering theoretical work by Mukamel and coworkers [37,148,149]. It can thus be expected that phase-sensitive spectroscopy applications making use of the temporal coherence properties provided by advanced FEL schemes will soon become an important tool for dynamic studies focusing on decoherence processes, entanglement and related phenomena such as quantum state tomography.

Furthermore, as the repetition rates of new FEL facilities are increasing by one to four orders of magnitude compared to the 'first-generation' FELs that operated with tens to a few hundreds of pulses per second (gas-phase pump-probe experiments at the European XFEL are now routinely performed with approximately 1000 pulses per second; and the currently ongoing upgrade to a superconducting accelerator at LCLS combined with an upgrade of the pump-probe lasers will soon enable time-resolved experiments with 30 to 100 kHz and eventually with up to 1 MHz), the required acquisition times for pump-probe experiments will decrease enormously, enabling more systematic explorations, e.g. of the dependence of atomic and molecular dynamics on the pump-pulse parameters. It also promises to be a game-changing advance for notoriously 'repetition-rate hungry' multi-particle coincidence experiments and other 'multi-messenger' approaches. Indeed, only very few electron-ion coincidence experiments, for example, have been performed with FELs to date [82,83,150,151]. The increased repetition rates combined with dedicated multi-particle coincidence end-station such as the reaction microscope at the SQS instrument at the European XFEL or the DREAM end-station at the TMO instrument at LCLS will finally make this powerful method a viable option for time-resolved experiments. It will also enable time-resolved Coulomb explosion imaging experiments performed in a multi-particle coincidence mode [117–119,152,153], as briefly mentioned in section III D 1. While the full 1-MHz repetition rate of LCLS-II might be challenging for ion-time-of-flight-based experiments since it only allows for a 1-microsecond detection window between subsequent X-ray pulses, thus severely limiting the achievable mass and momentum resolution, a 100-kHz repetition rate – corresponding to a 10-microsecond detection window – will most likely be ideal for these experiments.

In addition to the advances on the accelerator and X-ray side, another important development for pump-probe experiments is the push to provide more flexible wavelengths and shorter pulse durations for the external pump laser pulse. Combined with the need for higher repetition rates to match those of the FEL sources, this poses a formidable challenge for conventional laser technology and has therefore continuously risen in the R&D priorities at FEL facilities. Indeed, several recent experiments, most of them still unpublished to date, have used pump-pulses in the visible or UV produced by an OPA or few-cycle NIR pulses produced in a hollow-core fiber compressor. Some experiments have even been performed combining high harmonic generation with FELs [154,155]. All of these developments promise a bright future and exciting years ahead for FEL-based experiments exploring electronic and nuclear dynamics in gas-phase atoms and molecules.

Acknowledgments

I gratefully acknowledge the staff of FLASH, LCLS, SACLA, FERMI, the European XFEL, and SwissFEL for their tireless support and warm hospitality during the countless beamtimes I enjoyed at their facilities; and the many co-workers and collaborators over the years, who have made these FEL beamtimes successful and memorable experiences.

Disclosure statement

No potential conflict of interest was reported by the author(s).

Funding

This work was supported by the Chemical Sciences, Geosciences, and Biosciences Division, Office of Basic Energy Sciences, Office of Science, US Department of Energy, award no. DE-FG02-86ER13491.

References

[1] Pellegrini C, Stöhr J. X-ray free-electron lasers—principles, properties and applications, Nucl. Instrum Methods. Phys Res Sect A. 2003;500:33.
[2] Ackermann W, Asova G, Ayvazyan V, et al. Operation of a free-electron laser from the extreme ultraviolet to the water window. Nat Photon. 2007;1:336.
[3] Shintake T, Tanaka H, Hara T, et al. A compact free-electron laser for generating coherent radiation in the extreme ultraviolet region. Nat Photon. 2008;2:555.
[4] McNeil BWJ, Thompson NR. X-ray free-electron lasers. Nat Photon. 2010;4:814.
[5] Emma P, Akre R, Arthur J, et al. First lasing and operation of an ångstrom-wavelength free-electron laser. Nat Photon. 2010;4:641.
[6] Allaria E, Appio R, Badano L, et al. Highly coherent and stable pulses from the Fermi seeded free-electron laser in the extreme ultraviolet. Nat Photon. 2012;6:699.
[7] Ishikawa T, Aoyagi H, Asaka T, et al. A compact x-ray free-electron laser emitting in the sub ångström region. Nat Photon. 2012;6:540.
[8] Waldrop MM. X-ray science: the big guns. Nature. 2014;505:604.
[9] Pellegrini C, Marinelli A, Reiche S. The physics of x-ray free-electron lasers. Rev Mod Phys. 2016;88:015006.
[10] Pellegrini C. X-ray free-electron lasers: from dreams to reality. Phys Scr. 2016;2016:014004.
[11] Feng C, Wang Z, Wang X, et al. Generation of two-color ultra-short radiation pulses from two electron bunches and a chirped seeded free-electron laser. Nucl Instrum Methods Phys Res A. 2016;807:79–85.
[12] Milne CJ, Schietinger T, Aiba M, et al. The Swiss x-ray free electron laser. Appl Sci. 2017;7:720.
[13] Seddon EA, Clarke JA, Dunning DJ, et al. Short-wavelength free-electron laser sources and science: a review. Rep Prog Phys. 2017;80:115901.
[14] Ko IS, Kang H-S, Heo H, et al. Construction and commissioning of PAL-XFEL facility. Appl Sci. 2017;7:479.
[15] Kang H-S, Min C-K, Heo H, et al. Hard x-ray free-electron laser with femtosecond-scale timing jitter. Nat Photon. 2017;11:708.

[16] Decking W, Abeghyan S, Abramian P, et al. A MHz-repetition-rate hard x-ray free-electron laser driven by a superconducting linear accelerator. Nat Photonics. 2020;14:391–397.
[17] Liu B, Feng C, Gu D, et al. The SXFEL upgrade: from test facility to user facility. Appl Sci. 2021;12:176.
[18] Zewail AH. Femtochemistry: atomic-scale dynamics of the chemical bond using ultrafast lasers, Angew. Chem, Int Ed. 2000;39:2586.
[19] Amann J, Berg W, Blank V, et al. Demonstration of self-seeding in a hard-x-ray free-electron laser. Nat Photonics. 2012;6:693–698.
[20] Wöstmann M, Mitzner R, Noll T, et al. The XUV split-and-delay unit at beamline BL2 at FLASH. J Phys B. 2013;46:164005.
[21] Usenko S, Przystawik A, Lazzarino L, et al. Split-and-delay unit for FEL interferometry in the XUV spectral range. Appl Sci. 2017;7:544.
[22] Schmid G, Schnorr K, Augustin S, et al. Reaction microscope endstation at FLASH2. J Synchrotron Radiat. 2019;26:854–867.
[23] Berrah N. Molecular dynamics induced by short and intense x-ray pulses from the LCLS. Phys Scr. 2016;T169:014001.
[24] Jiang YH, Pfeifer T, Rudenko A, et al. Temporal coherence effects in multiple ionization of N_2 via XUV pump-probe autocorrelation. Phys Rev A. 2010;82:041403 (R).
[25] Chapman HN, Hau-Riege SP, Bogan MJ, et al. Femtosecond time-delay x-ray holography. Nature. 2007;448:676.
[26] Sauppe M, Rompotis D, Erk B, et al. XUV double-pulses with femtosecond to 650 ps separation from a multilayer-mirror- based split-and-delay unit at FLASH. J Synchrotron Radiat. 2018;25:1517–1528.
[27] Lutman AA, Coffee R, Ding Y, et al. Experimental demonstration of femtosecond two-color x-ray free-electron lasers. Phys Rev Lett. 2013;110:134801.
[28] Marinelli A, Ratner D, Lutman AA, et al. High-intensity double-pulse x-ray free-electron laser. Nat Commun. 2015;6:6369.
[29] Coffee RN, Cryan JP, Duris J, et al. Development of ultrafast capabilities for x-ray free-electron lasers at the Linac Coherent Light Source. Philos Trans R Soc A Math Phys Eng Sci. 2019;377:20180386.
[30] Zhang Y, Kroll T, Weninger C, et al., Generation of intense phase-stable femtosecond hard x-ray pulse pairs, Proceedings of the National Academy of Sciences **119**, e2119616119 (2022).
[31] Picón A, Lehmann CS, Bostedt C, et al. Hetero-site-specific x-ray pump-probe spectroscopy for femtosecond intramolecular dynamics. Nat Commun. 2016;7:11652.
[32] Prince KC, Allaria E, Callegari C, et al. Coherent control with a short-wavelength free-electron laser. Nat Photon. 2016;10:176.
[33] Maroju PK, Grazioli C, Di Fraia M, et al. Attosecond pulse shaping using a seeded free-electron laser. Nature. 2020;578:386–391.
[34] You D, Ueda K, Gryzlova EV, et al. New method for measuring angle-resolved phases in photoemission. Phys Rev X. 2020;10:031070.
[35] Callegari C, Grum-Grzhimailo AN, Ishikawa KL, et al. Atomic, molecular and optical physics applications of longitudinally coherent and narrow bandwidth free-electron lasers. Phys Rep. 2021;904:1–59.
[36] Wituschek A, Bruder L, Allaria E, et al. Tracking attosecond electronic coherences using phase-manipulated extreme ultraviolet pulses. Nat Commun. 2020;11:883.

[37] Mukamel S, Healion D, Zhang Y, et al. Multidimensional attosecond resonant x-ray spectroscopy of molecules: lessons from the optical regime. Annu Rev Phys Chem. 2013;64:101.
[38] Rolles D, Boll R, Erk B, et al. An experimental protocol for femtosecond NIR/UV - XUV pump-probe experiments with free-electron lasers. J Visualized Exp. 2018;140: e57055–e57055.
[39] Glownia JM, Cryan J, Andreasson J, et al. Time-resolved pump-probe experiments at the LCLS. Opt Express. 2010;18:17620.
[40] Redlin H, Al-Shemmary A, Azima A, et al. The FLASH pump–probe laser system: setup, characterization and optical beamlines. Nucl Instrum Methods Phys Res, Sect A. 2011;635.:S88–S93.
[41] Löhl F, Arsov V, Felber M, et al. Electron bunch timing with femtosecond precision in a superconducting free- electron laser. Phys Rev Lett. 2010;104:144801.
[42] Schulz S, Grguraš I, Behrens C, et al. Femtosecond all-optical synchronization of an x-ray free-electron laser. Nat Commun. 2015;6:5938.
[43] Savelyev E, Boll R, Bomme C, et al. Jitter-correction for IR/UV-XUV pump-probe experiments at the FLASH free-electron laser. New J Phys. 2017;19:043009.
[44] Hartmann N, Helml W, Galler A, et al. Sub-femtosecond precision measurement of relative x-ray arrival time for free-electron lasers. Nat Photonics. 2014;8:706–709.
[45] Frühling U, Wieland M, Gensch M, et al. Single-shot terahertz-field-driven x-ray streak camera. Nat Photon. 2009;3:523.
[46] Drescher M, Frühling U, Krikunova M, et al. Time- diagnostics for improved dynamics experiments at XUV FELs. J Phys B At Mol Opt Phys. 2010;43:194010.
[47] Meyer M, Costello JT, Düsterer S, et al. Two-colour experiments in the gas phase. J Phys B At Mol Opt Phys. 2010;43:194006.
[48] Düsterer S, Rehders M, Al-Shemmary A, et al. Development of experimental techniques for the characterization of ultrashort photon pulses of extreme ultraviolet free-electron lasers. Phys Rev ST Accel Beams. 2014;17:120702.
[49] Meyer M, Cubaynes D, O'Keeffe P, et al. Two-color photoionization in XUV free-electron and visible laser fields. Phys Rev A. 2006;74:011401.
[50] Radcliffe P, Düsterer S, Azima A, et al. Single-shot characterization of independent femtosecond extreme ultraviolet free electron and infrared laser pulses. Appl Phys Lett. 2007;90:131108.
[51] Meyer M, Cubaynes D, Richardson V, et al. Two-photon excitation and relaxation of the $3d - 4d$ resonance in atomic Kr. Phys Rev Lett. 2010;4:213001.
[52] Meyer M, Cubaynes D, Dardis J, et al. Two-color experiments in the gas phase at FLASH. J Electron Spectrosc Relat Phenom. 2010;181:111.
[53] Meyer M, Radcliffe P, Tschentscher T, et al. Angle-resolved electron spectroscopy of laser-assisted auger decay induced by a few-femtosecond x-ray pulse. Phys Rev Lett. 2012;108:063007.
[54] Düsterer S, Rading L, Johnsson P, et al. Interference in the angular distribution of photoelectrons in superimposed XUV and optical laser fields. J Phys B At Mol Opt Phys. 2013;46:164026.
[55] Düsterer S, Hartmann G, Bomme C, et al. Two-color XUV+NIR femtosecond photoionization of neon in the near-threshold region. New J Phys. 2019;21:063034.
[56] Düsterer S, Radcliffe P, Bostedt C, et al. Femtosecond x-ray pulse length characterization at the linac coherent light source free-electron laser. New J Phys. 2011;13:093024.
[57] Drescher M, Hentschel M, Kienberger R, et al. Time-resolved atomic inner-shell spectroscopy. Nature. 2002;419:803.

[58] Grguraš I, Maier AR, Behrens C, et al. Ultrafast x-ray pulse characterization at free-electron lasers. Nat Photon. 2012;6:852.
[59] Helml W, Maier AR, Schweinberger W, et al. Measuring the temporal structure of few-femtosecond free-electron laser x-ray pulses directly in the time domain. Nat Photonics. 2014;8:950–957.
[60] Hartmann N, Hartmann G, Heider R, et al. Attosecond time–energy structure of x-ray free-electron laser pulses. Nat Photon. 2018;12:215.
[61] Haynes DC, Wurzer M, Schletter A, et al. Clocking Auger electrons. Nat Phys. 2021.
[62] Ivanov R, Bermúdez Macias IJ, Liu J, et al. Single-shot temporal characterization of XUV pulses with duration from 10 fs to 350 fs at FLASH. J Phys B. 2020;53:184004.
[63] Wieland M, Kabachnik NM, Drescher M, et al. Deriving x-ray pulse duration from center-of-energy shifts in THz-streaked ionized electron spectra. Opt Express. 2021;29:32739.
[64] Usenko S, Przystawik A, Jakob M, et al. Attosecond interferometry with self-amplified spontaneous emission of a free-electron laser. Nat Commun. 2017;8. DOI:10.1038/ncomms15626.
[65] Usenko S, Schwickert D, Przystawik A, et al. Auger electron wave packet interferometry on extreme timescales with coherent soft x-rays. J Phys B. 2020;53:244008.
[66] Stapelfeldt H, Seideman T. Colloquium: aligning molecules with strong laser pulses. Rev Mod Phys. 2003;75:543.
[67] Johnsson P, Rouzée A, Siu W, et al. Field-free molecular alignment probed by the free electron laser in Hamburg (FLASH). J Phys B At Mol Opt Phys. 2009;42:134017.
[68] Cryan JP, Glownia JM, Andreasson J, et al. Auger electron angular distribution of double core-hole states in the molecular reference frame. Phys Rev Lett. 2010;105:083004.
[69] Rouzée A, Johnsson P, Rading L, et al. Towards imaging of ultrafast molecular dynamics using FELs. J Phys B At Mol Opt Phys. 2013;46:164029.
[70] Rolles D, Boll R, Adolph M, et al. Femtosecond x-ray photoelectron diffraction on gas-phase dibromobenzene molecules. J Phys B At Mol Opt Phys. 2014;47:124035.
[71] Küpper J, Stern S, Holmegaard L, et al. X-ray diffraction from isolated and strongly aligned gas-phase molecules with a free-electron laser. Phys Rev Lett. 2014;112:083002.
[72] Boll R, Anielski D, Bostedt C, et al. Femtosecond photoelectron diffraction on laser-aligned molecules: towards time-resolved imaging of molecular structure. Phys Rev A. 2013;88:061402(R.
[73] Boll R, Rouzée A, Adolph M, et al. Imaging molecular structure through femtosecond photoelectron diffraction on aligned and oriented gas-phase molecules. Faraday Discuss. 2014;171:57.
[74] Amini K, Boll R, Lauer A, et al. Alignment, orientation, and Coulomb explosion of difluoroiodobenzene studied with the pixel imaging mass spectrometry (PImMS) camera. J Chem Phys. 2017;147:013933.
[75] Kierspel T, Wiese J, Mullins T, et al. Strongly aligned gas-phase molecules at free-electron lasers. J Phys B At Mol Opt Phys. 2015;48:204002.
[76] Kierspel T, Morgan A, Wiese J, et al. X-ray diffractive imaging of controlled gas-phase molecules: toward imaging of dynamics in the molecular frame. J Chem Phys. 2020;152:084307.
[77] Boll R. *Imaging Molecular Structure with Photoelectron Diffraction*, Ph.D. thesis, Universität Heidelberg (2014).
[78] Anielski D. *Untersuchung der Photoelektronen-Winkelverteilungen von ausgerichteten Molekuelen in der Gasphase*, Ph.D. thesis, Universität Hamburg (2020).

[79] Kazama M, Fujikawa T, Kishimoto N, et al. Photoelectron diffraction from single oriented molecules: towards ultrafast structure determination of molecules using x-ray free-electron lasers. Phys Rev A. 2013;87:063417.
[80] Nakajima K, Teramoto T, Akagi H, et al. Photoelectron diffraction from laser-aligned molecules with x-ray free-electron laser pulses. Sci Rep. 2015;5:14065.
[81] Minemoto S, Shimada H, Komatsu K, et al. Time-resolved photoelectron angular distributions from nonadiabatically aligned CO_2 molecules with SX-FEL at SACLA. J Phys Comm. 2018;2:115015.
[82] Kastirke G, Schöffler MS, Weller M, et al. Double core-hole generation in O_2 molecules using an x-ray free-electron laser: molecular-frame photoelectron angular distributions. Phys Rev Lett. 2020;125:163201.
[83] Kastirke G, Schöffler MS, Weller M, et al. Photoelectron diffraction imaging of a molecular breakup using an x-ray free-electron laser. Phys Rev X. 2020;10:021052.
[84] Schoenlein R, Boutet S, Minitti M, et al. The Linac Coherent Light Source: recent developments and future plans. Appl Sci (Switzerland). 2017;7:10.3390/app7080850.
[85] Rudenko A, Inhester L, Hanasaki K, et al. Femtosecond response of polyatomic molecules to ultra-intense hard x-rays. Nature. 2017;546:129.
[86] Erk B, Boll R, Trippel S, et al. Imaging charge transfer in iodomethane upon x-ray photoabsorption. Science. 2014;345:288.
[87] Allum F, Anders N, Brouard M, et al. Multi-channel photodissociation and XUV-induced charge transfer dynamics in strong-field-ionized methyl iodide studied with time-resolved recoil-frame covariance imaging. Faraday Discuss. 2021;228:571–596.
[88] Cheng Y-C, Oostenrijk B, Lahl J, et al. Imaging multiphoton ionization dynamics of CH_3I at a high repetition rate XUV free-electron laser. J Phys B. 2021;54:014001.
[89] Boll R, Erk B, Coffee R, et al. Charge transfer in dissociating iodomethane and fluoromethane molecules ionized by intense femtosecond x-ray pulses. Struct Dyn. 2016;3:043207.
[90] Amini K, Savelyev E, Braußе F, et al. Photodissociation of aligned CH_3I and $C_6H_3F_2I$ molecules probed with time-resolved Coulomb explosion imaging by site- selective extreme ultraviolet ionization. Struct Dyn. 2018;5:014301.
[91] Braußе F, Goldsztejn G, Amini K, et al. Time-resolved inner-shell photoelectron spectroscopy: from a bound molecule to an isolated atom. Phys Rev A. 2018;97:043429.
[92] Forbes R, Allum F, Bari S, et al. Time-resolved site-selective imaging of predissociation and charge transfer dynamics: the CH_3I B-band. J Phys B. 2020;53:224001.
[93] Schnorr K, Senftleben A, Kurka M, et al. Electron rearrangement dynamics in dissociating I_2^{n+} molecules accessed by extreme ultraviolet pump-probe experiments. Phys Rev Lett. 2014;113:073001.
[94] Schnorr K, Senftleben A, Schmid G, et al. Multiple ionization and fragmentation dynamics of molecular iodine studied in IR-XUV pump-probe experiments. Faraday Discuss. 2014;171:41.
[95] Fisher-Levine M, Boll R, Ziaee F, et al. Time-resolved ion imaging at free-electron lasers using TimepixCam. J Synchrotron Radiat. 2018;25:336–345.
[96] Köckert H, Lee J, Allum F, et al. UV-induced dissociation of CH_2BrI probed by intense femtosecond XUV pulses. J Phys B. 2022;55:014001.
[97] Yong H, Xu X, Ruddock JM, et al., Ultrafast x-ray scattering offers a structural view of excited-state charge transfer, Proceedings of the National Academy of Sciences **118**, e2021714118 (2021).

[98] Ding T, Rebholz M, Aufleger L, et al. Nonlinear coherence effects in transient-absorption ion spectroscopy with stochastic extreme-ultraviolet free-electron laser pulses. Phys Rev Lett. 2019;123:103001.
[99] Rebholz M, Ding T, Despré V, et al. All-XUV pump-probe transient absorption spectroscopy of the structural molecular dynamics of di-iodomethane. Phys Rev X. 2021;11:031001.
[100] Fang L, Osipov T, Murphy BF, et al. Probing ultrafast electronic and molecular dynamics with free-electron lasers. J Phys B At Mol Opt Phys. 2014;47:124006.
[101] Rudenko A, Rolles D. Time-resolved studies with FELs. J Electron Spectrosc Relat Phenom. 2015;204:228.
[102] Takanashi T, Golubev N, Callegari C, et al. Time-resolved measurement of interatomic Coulombic decay induced by two-photon double excitation of Ne_2. Phys Rev Lett. 2017;118. DOI:10.1103/PhysRevLett.118.033202.
[103] Kumagai Y, Jurek Z, Xu W, et al. Real-time observation of disintegration processes within argon clusters ionized by a hard-x-ray pulse of moderate fluence. Phys Rev A. 2020;101:023412.
[104] Fukuzawa H, Takanashi T, Kukk E, et al. Real-time observation of x-ray-induced intramolecular and interatomic electronic decay in CH_2I_2. Nat Commun. 2019;10:2186.
[105] Krikunova M, Maltezopoulos T, Wessels P, et al. Ultrafast photofragmentation dynamics of molecular iodine driven with timed XUV and near-infrared light pulses. J Chem Phys. 2011;134:024313.
[106] Krikunova M, Maltezopoulos T, Wessels P, et al. Strong-field ionization of molecular iodine traced with XUV pulses from a free-electron laser. Phys Rev A. 2012;86:043430.
[107] Petrović VS, Siano M, White JL, et al. Transient x-ray fragmentation: probing a prototypical photoinduced ring opening. Phys Rev Lett. 2012;108:253006.
[108] Jiang YH, Senftleben A, Kurka M, et al. Ultrafast dynamics in acetylene clocked in a femtosecond XUV stopwatch. J Phys B At Mol Opt Phys. 2013;46:164027.
[109] Jiang YH, Rudenko A, Herrwerth O, et al. Ultrafast extreme ultraviolet induced isomerization of acetylene cations. Phys Rev Lett. 2010;105:263002.
[110] Liekhus-Schmaltz CE, Tenney I, Osipov T, et al. Ultrafast isomerization initiated by x-ray core ionization. Nat Commun. 2015;6:8199.
[111] Jiang YH, Rudenko A, Pérez-Torres JF, et al. Investigating two-photon double ionization of D_2 by XUV-pump–XUV-probe experiments. Phys Rev A. 2010;81:051402(R.
[112] Lehmann CS, Picón A, Bostedt C, et al. Ultrafast x-ray-induced nuclear dynamics in diatomic molecules using femtosecond x-ray-pump–x-ray-probe spectroscopy. Phys Rev A. 2016;94:013426.
[113] Schnorr K, Senftleben A, Kurka M, et al. Time-resolved measurement of interatomic coulombic decay in Ne_2. Phys Rev Lett. 2013;111:093402.
[114] Fang L, Xiong H, Kukk E, et al. X-ray pump-probe investigation of charge and dissociation dynamics in methyl iodine molecule. Appl Sci (Switzerland). 2017;7:10.3390/app7050529.
[115] Berrah N, Sanchez-Gonzalez A, Jurek Z, et al. Femtosecond-resolved observation of the fragmentation of buckminsterfullerene following x- ray multiphoton ionization. Nature Phys. 2019;15:1279.
[116] Krikunova M, Adolph M, Gorkhover T, et al. Ionization dynamics in expanding clusters studied by XUV pump–probe spectroscopy. J Phys B At Mol Opt Phys. 2012;45:105101.

[117] Boll R, Schäfer JM, Richard B, et al. X-ray multiphoton-induced Coulomb explosion images complex single molecules. Nat Phys. 2022. DOI:10.1038/s41567-022-01507-0
[118] Li X, Rudenko A, Schöffler MS, et al. Coulomb explosion imaging of small polyatomic molecules with ultrashort x-ray pulses. Phys Rev Res. 2022;4:013029.
[119] Jahnke T, Guillemin R, Inhester L, et al. Inner-shell-ionization-induced femtosecond structural dynamics of water molecules imaged at an x-ray free-electron laser. Phys Rev X. 2021;11:041044.
[120] Stolow A, Bragg AE, Neumark DM. Femtosecond time-resolved photoelectron spectroscopy. Chem Rev. 2004;104:1719.
[121] Wernet P, Leitner T, Josefsson I, et al. Communication: direct evidence for sequential dissociation of gas-phase $Fe(CO)_5$ via a singlet pathway upon excitation at 266 nm. J Chem Phys. 2017;146:211103.
[122] Mayer D, Lever F, Picconi D, et al. Following excited-state chemical shifts in molecular ultrafast x-ray photoelectron spectroscopy. Nat Commun. 2022;13:198.
[123] McFarland BK, Farrell JP, Miyabe S, et al. Ultrafast x-ray Auger probing of photoexcited molecular dynamics. Nat Commun. 2014;5:4235.
[124] Wolf TJA, Myhre RH, Cryan JP, et al. Probing ultrafast $\pi^*/n\pi^*$ internal conversion in organic chromophores via K-edge resonant absorption. Nat Commun. 2017;8:29.
[125] Pathak S, Ibele LM, Boll R, et al. Tracking the ultraviolet-induced photochemistry of thiophenone during and after ultrafast ring opening. Nat Chem. 2020;12:795–800.
[126] Squibb RJ, Sapunar M, Ponzi A, et al. Acetylacetone photodynamics at a seeded free-electron laser. Nat Commun. 2018;9:63.
[127] Driver T, Li S, Champenois EG, et al. Attosecond transient absorption spooktroscopy: a ghost imaging approach to ultrafast absorption spectroscopy. Phys Chem Chem Phys. 2020;22:2704.
[128] Li S, Driver T, Haddad AA, et al. Two-dimensional correlation analysis for x-ray photoelectron spectroscopy. J Phys B. 2021;54:144005.
[129] Li S, Driver T, Alexander O, et al. Time-resolved pump–probe spectroscopy with spectral domain ghost imaging. Faraday Discuss. 2021;228:488.
[130] Gorkhover T, Adolph M, Rupp D, et al. Nanoplasma dynamics of single large xenon clusters irradiated with superintense x-ray pulses from the linac coherent light source free-electron laser. Phys Rev Lett. 2012;108:245005.
[131] Gorkhover T, Schorb S, Coffee R, et al. Femtosecond and nanometre visualization of structural dynamics in superheated nanoparticles. Nat Photon. 2016;10:93–97.
[132] Rupp D, Adolph M, Gorkhover T, et al. Identification of twinned gas phase clusters by single-shot scattering with intense soft x-ray pulses. New J Phys. 2012;14:055016.
[133] Ferguson KR, Bucher M, Gorkhover T, et al. Transient lattice contraction in the solid-to- plasma transition. Sci Adv. 2016;2:e1500837.
[134] Minitti M, Budarz J, Kirrander A, et al. Imaging molecular motion: femtosecond x-ray scattering of an electrocyclic chemical reaction. Phys Rev Lett. 2015;114:255501.
[135] Glownia J, Natan A, Cryan J, et al. Self-referenced coherent diffraction x-ray movie of ångstrom- and femtosecond-scale atomic motion. Phys Rev Lett. 2016;117:153003.
[136] Stankus B, Yong H, Zotev N, et al. Ultrafast x-ray scattering reveals vibrational coherence following Rydberg excitation. Nat Chem. 2019;11:716–721.
[137] Yong H, Zotev N, Ruddock JM, et al. Observation of the molecular response to light upon photoexcitation. Nat Commun. 2020;11:2157.
[138] Bucksbaum PH, Ware MR, Natan A, et al. Characterizing multiphoton excitation using time-resolved x-ray scattering. Phys Rev. 2020;X **10**:011065.
[139] Ruddock JM, Yong H, Stankus B, et al. A deep UV trigger for ground-state ring-opening dynamics of 1,3-cyclohexadiene. Sci Adv. 2019;5:eaax6625.

[140] Young L, Ueda K, Gühr M, et al. Roadmap of ultrafast x-ray atomic and molecular physics. J Phys B At Mol Opt Phys. 2018;51:032003.
[141] Ueda K, Sokell E, Schippers S, et al. Roadmap on photonic, electronic and atomic collision physics: i. light–matter interaction. J Phys B. 2019;52:171001.
[142] Marinelli A, MacArthur J, Emma P, et al. Experimental demonstration of a single-spike hard-x-ray free-electron laser starting from noise. Appl Phys Lett. 2017;111:151101.
[143] Duris J, Li S, Driver T, et al. Tunable isolated attosecond x-ray pulses with gigawatt peak power from a free-electron laser. Nat Photon. 2020;14:30.
[144] Schwickert D, Ruberti M, Kolorenc P, et al. Electronic quantum coherence in glycine molecules probed with ultrashort x-ray pulses in real time. Sci Adv. 2022;8:eabn6848.
[145] Barillot T, Alexander O, Cooper B, et al. Correlation-driven transient hole dynamics resolved in space and time in the isopropanol molecule. Phys Rev X. 2021;11:031048.
[146] O'Neal JT, Champenois EG, Oberli S, et al. Electronic population transfer via impulsive stimulated x-ray Raman scattering with attosecond soft-x- ray pulses. Phys Rev Lett. 2020;125:073203.
[147] Li S, Driver T, Rosenberger P, et al. and J. P. Cryan, Attosecond coherent electron motion in Auger-Meitner decay. Science. 2022;375:285–290.
[148] Kowalewski M, Bennett K, Dorfman KE, et al. Catching conical intersections in the act: monitoring transient electronic coherences by attosecond stimulated X-ray Raman signals. Phys Rev Lett. 2015;115. DOI:10.1103/PhysRevLett.115.193003.
[149] Kowalewski M, Bennett K, Rouxel JR, et al. Monitoring nonadiabatic electron-nuclear dynamics in molecules by attosecond streaking of photoelectrons. Phys Rev Lett. 2016;117. DOI:10.1103/PhysRevLett.117.043201.
[150] Kurka M, Rudenko A, Foucar L, et al. Two-photon double ionization of Ne by free-electron laser radiation: a kinematically complete experiment. J Phys B At Mol Opt Phys. 2009;42:141002.
[151] Li X, Inhester L, Osipov T, et al. Electron-ion coincidence measurements of molecular dynamics with intense x-ray pulses. Sci Rep. 2021;11:505.
[152] Erk B, Rolles D, Foucar L, et al. Ultrafast charge rearrangement and nuclear dynamics upon inner-shell multiple ionization of small polyatomic molecules. Phys Rev Lett. 2013;110:053003.
[153] Erk B, Rolles D, Foucar L, et al. Inner-shell multiple ionization of polyatomic molecules with an intense x-ray free-electron laser studied by coincident ion momentum imaging. J Phys B At Mol Opt Phys. 2013;46:164031.
[154] Appi E, Papadopoulou CC, Mapa JL, et al. *et al.*, A synchronized VUV light source based on high-order harmonic generation at FLASH. Sci Rep. 2020;10:6867.
[155] Troß J, Pathak S, Summers A, et al. High harmonic generation in mixed XUV and NIR fields at a free-electron laser. J Opt. 2022;24:025502.